

Novel Anticancer Mechanism of Chamuangone through the Inhibition of Oncogenic Protein-Driven Oxidative Stress

Woraya Thianthong¹, Thanyarat Srichainan², Boonya Shuntawiwat², Sahaphum Laprom², Petcharat Chiangsaen³, Sarinya Kongpetch^{4,5}, Kiattawee Choowongkamon^{6,7}, Pharkphoom Panichayupakaranant^{8,9}, Papavee Samatiwat^{1*}

Abstract

Objective: To evaluate the anticancer mechanisms of Chamuangone against cholangiocarcinoma (CCA) cells. **Methods:** Chamuangone was tested for cytotoxicity against KKU-100 and KKU-452 cells for 24 and 48 h. Apoptosis, cell proliferation, mitochondrial membrane potential, and intracellular reactive oxygen species (ROS) levels were assessed using Annexin V, Ki-67, JC-1 assays, and DCFH-DA fluorescence probe, respectively. Oncology proteins expression was measured. **Results:** Chamuangone inhibited CCA cell growth in a dose- and time- dependent manner, with IC50 values in KKU- 100 cells of 1.175 and 0.331 µg/mL at 24 and 48 hours, respectively; in KKU- 452 cells, the IC50 values were 1.208 and 0.428 µg/mL. Consequently, Chamuangone at 1.5 and 3.0 µg/mL effectively induced both early and late apoptosis in a statistically significant manner, which correlated with a marked reduction in cell proliferation, as evidenced by the decrease in Ki-67 positive populations to 49.04% and 17.02%, respectively. Chamuangone at concentrations of 0.75, 1.5, and 3.0 µg/mL significantly induced mitochondrial dysfunction by reducing the Red/Green fluorescence ratio across all time points (3–24 h), indicating a loss of mitochondrial membrane potential that triggers apoptosis. The induction of intracellular oxidative stress was indicated by a significant increase in the high-dose group of Chamuangone. Moreover, it also suppressed the expression of key ROS- and oxidative stress-associated oncogenic proteins, including Carbonic Anhydrase IX, Enolase2, CXCL8/IL-8, Galectin-3, EGFR/ErbB1, Progranulin, FGF basic, Dkk-1, p27/kip1, Mesothelin, Survivin, leading to redox imbalance and apoptosis in KKU-100 cells. **Conclusion:** Chamuangone inhibits CCA cell proliferation by inducing apoptosis through mechanisms involving the suppression of the Ki67, loss of mitochondrial membrane potential, intracellular ROS accumulation, and downregulation of oncogenic-related proteins involved in proliferation, survival, angiogenesis, and oxidative stress. Thus, Chamuangone has significant potential as a lead compound for the development of novel CCA therapeutics.

Keywords: Cholangiocarcinoma- Anticancer- Chamuangone- Oxidative stress- Oncogenic proteins

Asian Pac J Cancer Prev, 27 (6), 2189-2201

Introduction

Cholangiocarcinoma (CCA) is a malignant epithelial tumor arising from the bile ducts and is the second most common primary hepatic malignancy worldwide. Although its global incidence is generally less than 2 per 100,000 and its accounts for approximately 3% of gastrointestinal cancers, rates vary markedly by geography, with the highest incidence reported in

parts of East and Southeast, especially in northeastern Thailand where incidence can reach up to 85 per 100,000 [1]. These established risk factors in endemic regions, including infection with the hepatobiliary flukes such as *Opisthorchis viverrini* and *Clonorchis sinensis* which induce chronic biliary inflammation and are classified carcinogens, as well as hepatolithiasis, which can drive secondary chronic inflammation [2]. Additional risk factors include choledochal cysts, primary sclerosing

¹Department of Pharmacology, Faculty of Medicine, Srinakharinwirot University, Bangkok, Thailand. ²Medical Degree Program, Faculty of Medicine, Srinakharinwirot University, Bangkok, Thailand. ³Department of Physiology, Faculty of Medicine, Srinakharinwirot University, Bangkok, Thailand. ⁴Department of Pharmacology, Faculty of Medicine, Khon Kaen University, Khon Kaen, Thailand. ⁵Cholangiocarcinoma Research Institute, Khon Kaen University, Khon Kaen, Thailand. ⁶Department of Biochemistry, Faculty of Science, Kasetsart University, Bangkok, Thailand. ⁷Center for Advanced Studies in Nanotechnology for Chemical, Food and Agricultural Industries, Kasetsart University Institute for Advanced Studies, Kasetsart University, Bangkok, Thailand. ⁸Department of Pharmacognosy and Pharmaceutical Botany, Faculty of Pharmaceutical Sciences, Prince of Songkla University, Songkhla, Thailand. ⁹Phytomedicine and Pharmaceutical Biotechnology Excellence Center, Faculty of Pharmaceutical Sciences, Prince of Songkla University, Songkhla, Thailand. *For Correspondence: papavees@g.swu.ac.th

cholangitis, and chronic virus hepatitis, among others [3]. Collectively, these factors imply chronic inflammation as a central driver of cholangiocarcinogenesis.

In instances of unresectable CCA or advanced CCA, the first-line therapeutic approach is chemotherapy utilizing gemcitabine in conjunction with a platinum-based agent [4, 5]. Nonetheless, clinical outcomes remain poor due to intrinsic and acquired drug resistance as well as profound inter- and intratumoral heterogeneity [6]. Regarding chemotherapy resistance, key molecular mechanisms alteration involves drug efflux, enhanced DNA damage repair (DDR), apoptosis evasion, epigenetic modifications, altered intracellular drug metabolism, and cancer stem cells (CSCs) dynamics [7]. Therefore, therapeutic strategies that interfere with critical molecular pathways, including oncogenic kinases involved in cancer progression, survival, migration and angiogenesis, may offer superior anticancer efficacy [8]. These challenges underscore the need for new therapeutic strategies and mechanistic insights.

Chamuangone is a polyprenylated benzophenone compound isolated from the leaves of *Garcinia cowa* (Chamuang), a plant wildy found in Thailand [9]. It has demonstrated antiproliferative effects in several cancer models [10-15]. However, its activity and underlying mechanisms in CCA remain incompletely characterized. Here, we investigate the anticancer effects of Chamuangone against CCA and explore its mechanisms of action. Specifically, we evaluate its impact on CCA cell viability and apoptosis and assess relevant oncogenic proteins implicated in CCA pathobiology and drug resistance. This study demonstrates the pharmacological profile of Chamuangone in CCA models, which will help guide complementary therapeutic strategies and provide a rationale for further preclinical evaluation.

Materials and Methods

Chemical Materials

Dimethyl sulfoxide (DMSO) and methanol were purchased from Merck (Darmstadt, Germany). 3-(4,5-Dimethylthiazol-2-yl)-2,5-diphenyltetrazolium bromide (MTT) was purchased from Sigma-Aldrich (St. Louis, MO, USA). Ham's F-12 medium, penicillin-streptomycin, Fetal bovine serum (FBS), and minimum essential medium (MEM) were purchased from GIBCO Invitrogen (Grand Island, NY, USA).

Extraction and Purification of Chamuangone from *Garcinia cowa* Leaves

Dried leaves of *Garcinia cowa* were powdered (1 kg) and extracted by microwave-assisted extraction using n-hexane. The extraction was performed at a microwave frequency of 2450 MHz with a power output of 600 W for three irradiation cycles, each consisting of 60 s of irradiation followed by 30 s of cooling. The extract was filtered and concentrated under reduced pressure at 40 °C to obtain the crude hexane extract [12]. Isolation of Chamuangone was carried out using a modified method based on previously reported procedures [10, 14]. The crude extract was further purified to yield Chamuangone

as a light yellowish oil. The identity and purity of the isolated compound were confirmed by nuclear magnetic resonance (NMR) spectroscopy, and the obtained spectral data were consistent with previously reported values for Chamuangone [14].

Cell Lines and Culture Conditions

This study employed two human cholangiocarcinoma (CCA) cell lines, KKU-100 (JCRB1568) [16] and KKU-452 (JCRB1772) [17], which were originally derived from Thai CCA patients with written informed consent obtained in accordance with protocols approved by Khon Kaen University [18, 19]. Both cell lines were obtained from the Japanese Cancer Research Resources Bank. All procedures were performed in accordance with previously established protocols for the maintenance of CCA cell lines [20, 21]. The cells were cultured in Ham's F-12 medium supplemented with 12.5 mM N-2-hydroxyethylpiperazine-N'-2-ethanesulfonic acid (HEPES, pH 7.3), 100 U/mL penicillin, 100 µg/mL streptomycin, and 10% fetal bovine serum (FBS), and maintained at 37 °C in a humidified atmosphere containing 5% CO₂. Cells were subcultured upon reaching 80-90% confluence every three days using 0.25% trypsin-EDTA to dissociate adherent monolayers, and the culture medium was replaced after overnight incubation. Cell viability was assessed via trypan blue exclusion prior to seed for assays. Cell seeding density was optimized to ensure logarithmic growth throughout the experimental period.

MTT assay

Cell lines were seeded into 96-well plates overnight to allow for cell attachment. Chamuangone was dissolved in DMSO and subsequently diluted in the culture medium to final concentrations ranging from 0 to 3 µg/ml (0, 0.1875, 0.375, 0.75, 1.5, and 3 µg/ml). Cells were treated with these concentrations for 24 and 48 h. In all experimental and control groups, the final concentration of DMSO vehicle was maintained at 0.1 % (v/v) [22]. Cytotoxic activity was evaluated using the 3-(4,5-dimethylthiazol-2-yl)-2,5-diphenyltetrazolium bromide (MTT) assay, as previously described [21]. Following the treatment period, cells were incubated with the MTT solution (5 mg/ml) at 37 °C for 4 h. The supernatant was then removed, and the resulting formazan crystals were dissolved in 100 µl of DMSO. The absorbance was measured at 540 nm using a SpectraMax M2 microplate reader. Cell viability was expressed as a percentage relative to the untreated control (defined as 100%). The half-maximal inhibitory concentration (IC₅₀) values were determined via nonlinear curve-fitting using Sigma Plot software (version 10.0).

Apoptosis Assay

KKU-100 cells were seeded into 6-well plates and allowed to adhere overnight. Apoptosis was induced by treating the cells with Chamuangone at concentrations of 0.75, 1.5, and 3.0 µg/mL for 24 and 48 h. Following treatment, cells were then harvested and stained using the Muse™ Annexin V & Dead Cell Kit (MCH100105, Luminex Corporation, Austin, TX, USA) according to the manufacturer's instructions and a previously

reported protocol [21]. The stained cell suspension was incubated for 20 minutes at room temperature in the dark. Subsequently, the percentages of live, early apoptotic, late apoptotic, and dead cells were analyzed using a Muse™ Cell Analyzer [23].

Cell Proliferation Analysis

Cell proliferation was evaluated using the Muse® *Ki67* Proliferation kit (MCH100114, Luminex Corporation, Austin, TX, USA) according to the manufacturer's instructions. K KU-100 cells were seeded into 6-well plates and allowed to adhere overnight. Cells were treated with Chamuangone at concentrations of 1.5 and 3.0 µg/mL for 24 h. Following treatment, cells were fixed and permeabilized using the fixation and permeabilization reagents provided in the kit. Cells were then stained with a primary antibody against Ki-67 for 1 hour at room temperature. The cells were washed three times with PBS, followed by incubation with a fluorescent dye-conjugated secondary antibody in the dark for 1 hour. The percentages of *Ki67*-positive (proliferating) and *Ki67*-negative (non-proliferating) cells were quantified using the Guava® Muse® cell analyzer [24].

JC-1 Assay for Mitochondrial Membrane Potential ($\Delta\psi_m$)

K KU-100 cells were seeded into 96-well plates and allowed to adhere overnight. Cells were then treated with 0.75, 1.5, and 3.0 µg/mL of Chamuangone for 3, 6, and 24 h to assess changes in $\Delta\psi_m$. The JC-1 dye (Sigma-Aldrich, St. Louis, MO, USA) was used for detecting fluorescence shift from green to red in response to changes in $\Delta\psi_m$. After treatment, cells were incubated with JC-1 dye prepared in serum-free medium (SFM) to make the final concentration at 2 µM at 37°C, 5% CO₂, for 15-20 minutes. The cells were then washed twice with PBS and replenished with 100 µL of SFM per well. Fluorescence intensity was measured using a Biotek Synergy HT microplate reader at excitation/emission wavelengths of 530 nm (green fluorescence) and 590 nm (red fluorescence). Cells with high mitochondrial membrane potential exhibited predominant red fluorescence, whereas cells with depolarized mitochondria showed increased green fluorescence. $\Delta\psi_m$ was quantitatively expressed as the ratio of red to green fluorescence, reflecting mitochondrial functional integrity [25].

Reactive Oxygen Species (ROS) Assay

K KU-100 cells were seeded in 96-well plates and incubated overnight to allow cell attachment. The cells were then treated with 3.0 µg/mL of Chamuangone for 3, 6, 24, and 48 h. At the indicated time points, the cells were washed twice with PBS and incubated with the stain. 2',7'-Dichlorofluorescein diacetate (DCFH-DA) (Sigma-Aldrich, St. Louis, MO, USA), which was dissolved in SFM to a final concentration of 10 µM for 30 minutes at 37°C in the dark. Subsequently, the cells were washed twice with PBS, and 100 µL of SFM was added to each well. Fluorescence intensity was measured using a Biotek Synergy HT microplate reader at an excitation wavelength of 485 nm and an emission wavelength of 530 nm to assess the levels of intracellular ROS [26]. The results

were expressed as the percentage change in ROS levels relative to the control group.

Protein Expression Analysis using Human XL Oncology Array

K KU-100 cells were treated with Chamuangone at a concentration of 3.0 µg/mL for 24 h. Protein was subsequently extracted from the cell lysates using a lysis buffer. The expression levels of oncology-related proteins were screened using the Proteome Profiler™ Human XL Oncology Array Kit (Cat. No. ARY026, R&D Systems, Minneapolis, MN, USA) according to the manufacturer's protocol. The protein spot densities were analyzed using a Uvitec Alliance Q9 Advanced Chemiluminescence Imager (UVITEC, Cambridge, UK). The expression levels of oncology-related proteins were normalized to the internal positive controls provided on the array membrane [27].

Statistical analysis

All data were presented as the mean ± standard deviation (SD) from at least three independent experiments. Statistical significance was analyzed using one-way analysis of variance (one-way ANOVA), followed by Student's t-test for pairwise comparisons. A p-value < 0.05 was considered statistically significant. All statistical data analyses were performed using GraphPad Prism software.

Results

Cytotoxic Effects of Chamuangone on Cholangiocarcinoma (CCA) Cells

K KU-100 and K KU-452 cells were used to evaluate the cytotoxic effects of Chamuangone at 24 and 48 h and to determine the IC₅₀ values. In K KU-100 cells, the IC₅₀ values were 1.175 µg/mL at 24 h and decreased to 0.331 µg/mL at 48 h. Similarly, in K KU-452 cells, the IC₅₀ values were 1.208 µg/mL and decreased to 0.428 µg/mL as shown in Table 1. These results indicate that Chamuangone significantly inhibited the growth of CCA cells in a time- and dose-dependent manner (Figure 1 A-B). Notably, Chamuangone exhibited greater cytotoxic potency in K KU-100 cells compared with K KU-452 cells, as evidenced by lower IC₅₀ values. Therefore, the K KU-100 cell line was selected for further experimental procedures.

Chamuangone Induces Apoptosis in CCA Cells

To determine whether Chamuangone induces programmed cell death, an apoptosis assay was performed. After treatment with Chamuangone at 3.0 µg/mL for 48 h, the percentage of live cells markedly decreased, while early apoptotic, late apoptotic, and dead cell populations significantly increased compared with the untreated control (Table 2). These results indicate that Chamuangone suppresses CCA cell growth through the induction of apoptosis in both early and late stages in a statistically significant, time-dependent manner (Figure 2 A-C). Collectively, the proportions of live, early apoptotic, late apoptotic, and dead K KU-100 cells following Chamuangone treatment clearly demonstrate a shift from viable cells toward apoptotic and dead cell populations,

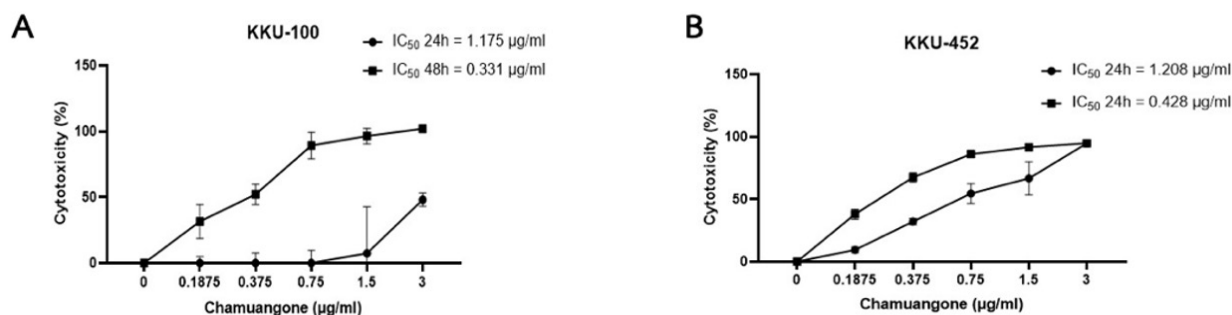


Figure 1. The Effect of Chamuangone on Cell Viability in KKU-100 and KKU-452 Cells. (A) KKU-100 and (B) KKU-452 cells were treated with various concentrations of Chamuangone (0.1875, 0.375, 0.75, 1.5, and 3.0 µg/mL) for 24 and 48 h. Cell viability was determined using the MTT assay. Data represent the mean ± SD (n=3). p < 0.05 compared with control.

Table 1. The IC₅₀ Values of Chamuangone on KKU-100 and KKU-452 Cells. KKU-100 and KKU-452 cells were treated with various concentrations of Chamuangone for 24 and 48 h. The IC₅₀ values were determined using the MTT assay.

IC ₅₀		KKU-100		KKU-452	
Bioactive compound	IC ₅₀ -24 h (µg/ml)	IC ₅₀ -48 h (µg/ml)	IC ₅₀ -24 h (µg/ml)	IC ₅₀ -48 h (µg/ml)	
Chamuangone	1.175 ± 0.47	0.331 ± 0.20	1.208 ± 0.13	0.428 ± 0.10	

confirming apoptosis as a key mechanism underlying the cytotoxic effects of Chamuangone in CCA cells.

Chamuangone Suppresses Ki67 Expression, a Marker of CCA Cell Proliferation

Ki67 expression was used to assess the proliferative activity of CCA cells. The results demonstrated that treatment with Chamuangone at concentrations of 1.5 and 3.0 µg/mL significantly decreased the percentage of Ki67-positive cells compared with the control group, while the proportion of Ki67-negative cells was correspondingly increased at 24 h (Figure 3A–B). The average relative ratio of Ki67-positive/Ki67-negative in the group treated with 1.5 µg/mL Chamuangone was 49.04%, and treatment with 3.0 µg/mL Chamuangone further reduced the ratio to 17.02%, representing a statistically significant, dose-dependent decrease (Table 3). These findings indicate that Chamuangone effectively suppresses CCA cell proliferation by reducing the proportion of actively cycling cells. The marked decrease in Ki67 expression suggests that Chamuangone induces cell cycle arrest and promotes

the transition of CCA cells into a non-proliferative (quiescent) state, thereby highlighting its potential as an anti-CCA agent through inhibition of cell division.

Chamuangone Alters Mitochondrial Membrane Potential (Δψm) in CCA cells

The JC-1 assay was employed to evaluate changes in Δψm. The JC-1 dye exhibits red fluorescence in mitochondria with intact membrane potential, whereas a shift toward green fluorescence indicates mitochondrial depolarization. The red/green fluorescence ratio was therefore used as an indicator of mitochondrial integrity. KKU-100 cells were treated with Chamuangone at concentrations of 0.75, 1.5, and 3.0 µg/mL for 3, 6, and 24 h. Chamuangone treatment resulted in a marked reduction in the red/green fluorescence ratio at all tested concentrations and time points compared with the control group, indicating disruption of mitochondrial membrane potential. At 3 h, the average red/green fluorescence ratios were reduced to 33.21, 35.06, and 32.25 following treatment with 0.75, 1.5, and 3.0 µg/mL Chamuangone,

Table 2. The percentage of live, early apoptotic, late apoptotic, and dead KKU-100 cells after Chamuangone treatment. KKU-100 cells were treated with 0.75, 1.5, and 3.0 µg/mL of Chamuangone for 24 and 48 h. The percentage of cells in each phase of apoptosis was determined using the Muse™ Annexin V & Dead Cell Kit. Data represent the mean ± SD (n=3), p < 0.05 compared with control.

Profile	24 h					48 h			
	% Gated of control	% Gated of Ch 0.75 µg/ml	% Gated of Ch 1.5 µg/ml	% Gated of Ch 3.0 µg/ml	% Gated of control	% Gated of Ch 0.75 µg/ml	% Gated of Ch 1.5 µg/ml	% Gated of Ch 3.0 µg/ml	
Mean Live (LL)	87.55	86.57	77.3*	40.45*	90.28	89.32	67.68*	32.08*	
Early Apoptotic (LR)	4.57	4.2	8.33*	18.17*	4.65	3.47	9.73*	27.87*	
Late Apop./Dead (UR)	3.52	3.52	8.20*	21.22*	2.45	2.92	10.50*	36.68*	
Debris (UL)	4.37	5.72	6.17*	20.17*	2.62	4.3	12.08*	3.37*	
Total Apoptotic	8.08	7.72	16.53*	39.39*	7.10	6.38	20.23*	64.55*	

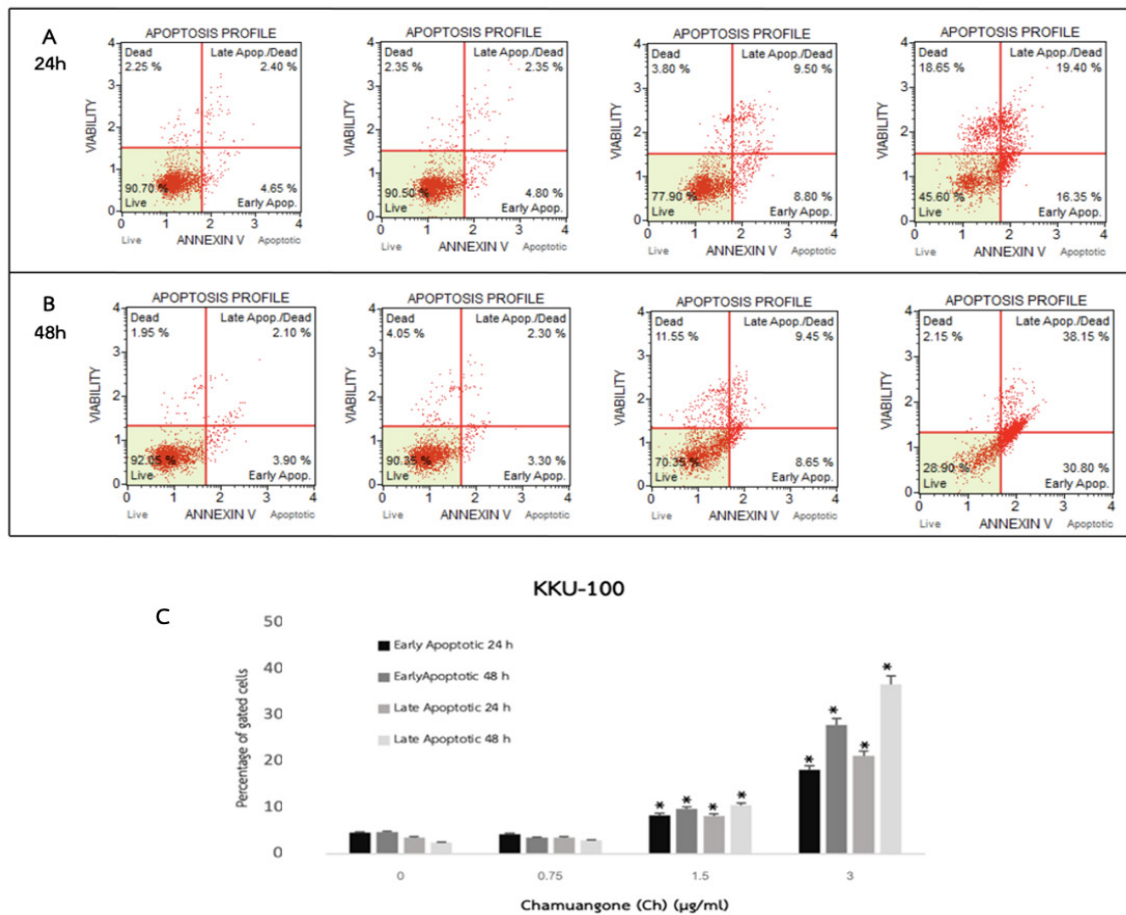


Figure 2. The Effect of Chamuangone on Apoptosis Induction in KKKU-100 Cells. (A) Flow cytometric plots showing live, early apoptotic, late apoptotic, and dead cells after treatment with 0.75, 1.5, and 3.0 µg/mL of Chamuangone for 24 h. (B) treatment with 0.75, 1.5, and 3.0 µg/mL of Chamuangone for 48 h. Using the Muse™ Annexin V & Dead Cell Kit. (C) Quantitative analysis showing the percentage of apoptotic and live cells. Data represent the mean ± SD (n=3). p < 0.05 compared with control.

respectively. At 6 h, the ratios were 62.24, 66.94, and 56.09 for the respective concentrations, while at 24 h, the ratios further decreased to 45.80, 43.83, and 44.45 (Table 4). All values were significantly lower than those of the control group. Representative fluorescence images were captured to compare mitochondrial staining patterns between control and treated cells (Figure 4 A-C). There were obvious changes in the fluorescence signal, reflecting the difference in the $\Delta\psi_m$ values of mitochondria. The results showed that at all concentrations and at all time points, the Red/Green ratio of Chamuangone-treated cells was significantly reduced compared to the control group (Figure 4 D). Therefore, these results indicate that Chamuangone induces mitochondrial membrane depolarization in CCA cells in a time- and concentration-independent manner within the tested range.

The loss of $\Delta\psi_m$ reflects mitochondrial dysfunction and supports the involvement of the mitochondrial pathway in Chamuangone-induced apoptosis.

Chamuangone Induces Intracellular Reactive Oxygen Species (ROS) in CCA cells

The study investigated the effect of Chamuangone on the induction of intracellular oxidative stress. KKKU-100 cells treated with 3.0 µg/mL of Chamuangone, and the results were collected at 3, 6, 24, and 48 hours, with the experiment repeated three times. The results showed that intracellular ROS levels increased in all treatment groups compared with the control (Table 5). Quantitative analysis further indicated that intracellular ROS levels were significantly increased following Chamuangone exposure at concentrations of 3.0 µg/mL, which exhibited the highest

Table 3. The Percentage of Ki67-Positive Cells in KKKU-100 after Chamuangone Treatment. KKKU-100 cells were treated with Chamuangone at 1.5 and 3.0 µg/mL for 24 h. The percentage of Ki67-positive proliferating cells was evaluated by immunofluorescence staining. Data represent the mean ± SD (n=3), p < 0.05 compared with control.

KKU-100 (24 h)		% Gated Negative Cells (Ki67-)	% Gated Proliferating Cells (Ki67+)	Ratio (Ki67+)/(Ki67-)	% Ratio (Ki67+)/(Ki67-)
Mean	Control	17.68	82.32	5.3	100
	Ch 1.5 µg/ml	31.15	68.85	2.34	49.04*
	Ch 3.0 µg/ml	64.63	35.37	0.62	17.02*

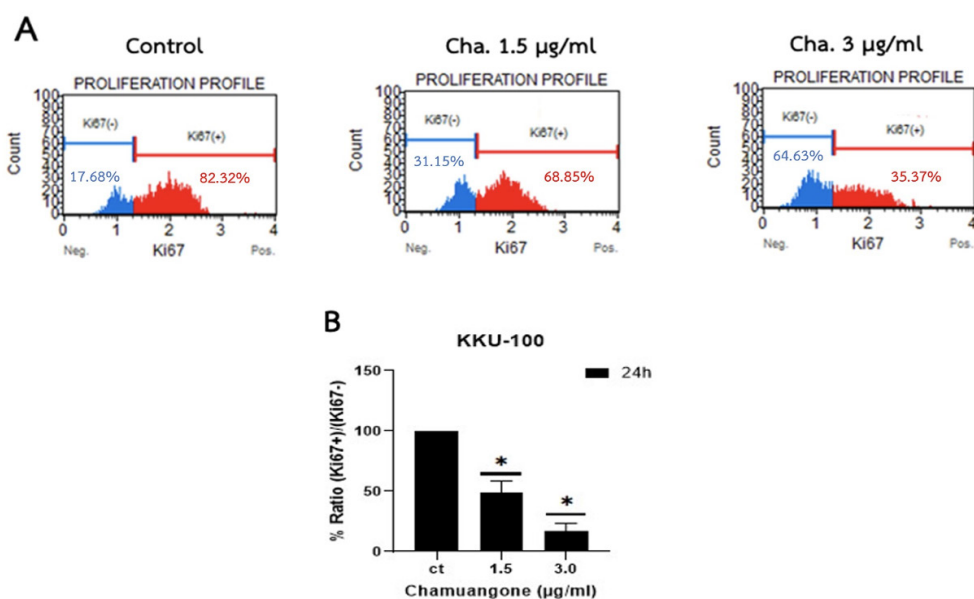


Figure 3. The Effect of Chamuangone on *Ki67* Expression in KKU-100 Cells. (A) Immunofluorescence images of *Ki67*-positive cells after treatment with 1.5 and 3.0 µg/mL of Chamuangone for 24 h. Nuclei were counterstained with DAPI. (B) Quantification of *Ki67*-positive cell percentage relative to total cells. Data represent the mean ± SD (n=3). $p < 0.05$ compared with control.

fluorescence signals at 6, 24, and 48 hours (Figure 5). This indicates that Chamuangone at higher concentrations can effectively induce oxidative stress in KKU-100 cells. The

results of this experiment demonstrated that Chamuangone can generate ROS and induces oxidative stress, which may contribute to mitochondrial dysfunction and subsequent

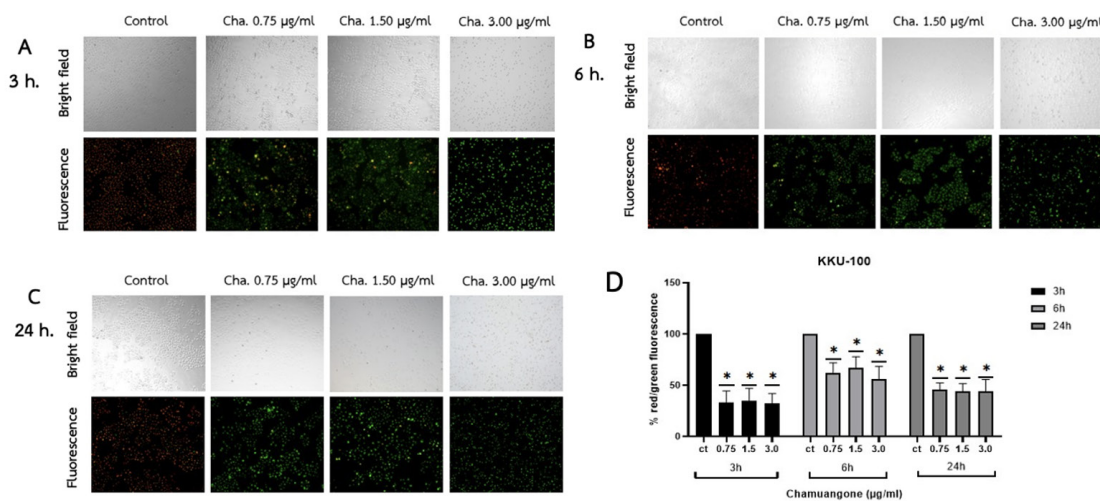


Figure 4. The Effect of Chamuangone on Mitochondrial Membrane Potential ($\Delta\psi_m$) in KKU-100 Cells. (A), (B), (C) Representative JC-1 fluorescence images showing the red (aggregated) and green (monomeric) signals at 3, 6, and 24 h after treatment with Chamuangone (0.75, 1.5, and 3.0 µg/mL). (D) Quantitative analysis of the red/green fluorescence ratio indicates mitochondrial depolarization. Data represent the mean ± SD (n=3). $p < 0.05$ compared with control.

Table 4. The Red/Green Fluorescence Ratio of KKU-100 Cells after Chamuangone Treatment. KKU-100 cells were treated with Chamuangone at 0.75, 1.5, and 3.0 µg/mL for 3, 6, and 24 h. The mitochondrial membrane potential was determined by JC-1 staining and expressed as the red/green fluorescence ratio. Data represent the mean ± SD (n=3), $p < 0.05$ compared with control.

JC1 assay	3 h				6 h				24 h			
	% Control	% Ch 0.75 µg/ml	% Ch 1.5 µg/ml	% Ch 3.0 µg/ml	% Control	% Ch 0.75 µg/ml	% Ch 1.5 µg/ml	% Ch 3.0 µg/ml	% Control	% Ch 0.75 µg/ml	% Ch 1.5 µg/ml	% Ch 3.0 µg/ml
Mean % red/green fluorescence	100	33.21*	35.06*	32.25*	100	62.24*	66.94*	56.09*	100	45.80*	43.83*	44.45*

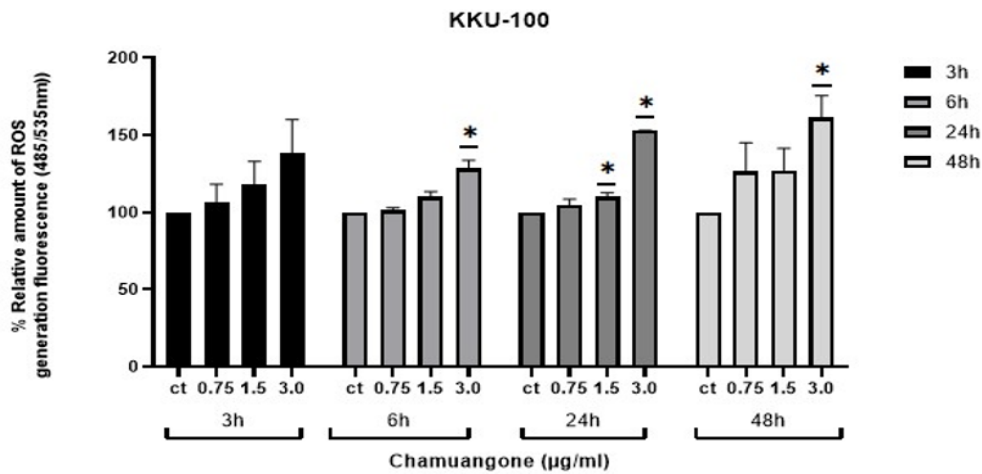


Figure 5. The Effect of Chamuangone on Intracellular Reactive Oxygen Species (ROS) Production in KKKU-100 Cells. Quantitative analysis of relative ROS fluorescence intensity compared with the control group. Data represent the mean \pm SD (n=3). $p < 0.05$ compared with control.

apoptosis.

Chamuangone Suppresses Human Oncogenic-Related Proteins

Given that higher concentrations of Chamuangone markedly increased intracellular ROS levels, we further investigated whether Chamuangone modulates oncogenic protein-driven oxidative stress using the Proteome Profiler™ Human XL Oncology Array, which simultaneously detects 84 cancer-related proteins. The results revealed that treatment of KKKU-100 cells with Chamuangone at 3.0 $\mu\text{g}/\text{mL}$ for 24 h significantly altered the expression profile of oncogenic proteins compared with the control group. Among the 84 proteins analyzed, 11 oncogenic-related proteins were markedly downregulated following Chamuangone treatment, including Carbonic Anhydrase IX, Enolase2, CXCL8/IL-8, Galectin-3, EGFR/ErbB1, Progranulin, FGF basic, Dkk-1, p27/kip1, Mesothelin, Survivin (Table 6). These proteins are well recognized for their roles in promoting cancer cell growth, survival, angiogenesis, metastasis, inflammation and resistance to apoptosis. Notably, FGF basic showed the most marked reduction among

all proteins analyzed, decreasing from a high basal expression level in control cells to nearly undetectable levels following Chamuangone treatment (Figure 6 A-B). In parallel, Chamuangone disrupts several oncogenic redox homeostasis-regulating proteins, including EGFR/ErbB1, CXCL8/IL-8, Galectin-3, Carbonic anhydrase IX, Enolase 2, and Survivin (Figure 6 A-B). Based on the protein array screening, key oncogenic and oxidative stress-associated proteins were identified as potential targets of Chamuangone. These findings were further supported by functional assays demonstrating increased ROS production, mitochondrial membrane depolarization, and apoptosis, suggesting a consistent mechanistic link between oncogenic protein suppression and Chamuangone-induced cytotoxicity.

Discussion

Based on the experimental results of this research, Chamuangone exerts potent anticancer effects against cholangiocarcinoma (CCA) cells through the suppression of cell viability, demonstrating potent dose- and time-dependent inhibitory effects. Notably, KKKU-100 cells

Table 5. The Relative Fluorescence Intensity of ROS in KKKU-100 Cells after Chamuangone Treatment. KKKU-100 Cells were Treated with 3.0 $\mu\text{g}/\text{mL}$ of Chamuangone and Measured at 3, 6, 24, and 48 h. Intracellular ROS generation was detected using DCFH-DA staining. Data represent the mean \pm SD (n=3), $p < 0.05$ compared with control.

	3 h				6 h			
	% Ct	% Ch 0.75 $\mu\text{g}/\text{ml}$	% Ch 1.5 $\mu\text{g}/\text{ml}$	% Ch 3.0 $\mu\text{g}/\text{ml}$	% Ct	% Ch 0.75 $\mu\text{g}/\text{ml}$	% Ch 1.5 $\mu\text{g}/\text{ml}$	% Ch 3.0 $\mu\text{g}/\text{ml}$
% Relative amount of ROS generation fluorescence (485/535nm)	100	106.83	118.36	138.45	100	101.26	109.98	128.49*
	24 h				48 h			
	% Ct	% Ch 0.75 $\mu\text{g}/\text{ml}$	% Ch 1.5 $\mu\text{g}/\text{ml}$	% Ch 3.0 $\mu\text{g}/\text{ml}$	% Control	% Ch 0.75 $\mu\text{g}/\text{ml}$	% Ch 1.5 $\mu\text{g}/\text{ml}$	% Ch 3.0 $\mu\text{g}/\text{ml}$
% Relative amount of ROS generation fluorescence (485/535nm)	100	104.83	109.93*	152.73*	100	126.35	127.16	161.34*

were more sensitive to Chamuangone than KKU-452 cells. Differential sensitivity of CCA subtypes to Chamuangone which exhibit distinct molecular and clinical characteristics, often influencing their susceptibility to various therapeutic agents [28]. The KKU-100 cell line was established from a well-differentiated intrahepatic cholangiocarcinoma derived from a male patient infected with *Opisthorchis viverrini* in Thailand. This cell line exhibits epithelial-like morphology, moderate proliferation with a doubling time of approximately 38 hours, and moderate migratory and invasive abilities. KKU 452 is a poorly differentiated adenocarcinoma with a 17.9 h doubling time, and fast migration and invasion properties with high expression of N-cadherin and TP53 mutation [17]. The molecular heterogeneity of CCA further differences between live fluke- and non-live fluke-associated such as KRAS, G12D, and TP53 alteration and contribute to resistance therapy in CCA [28-30]. Previous studies have also demonstrated that Chamuangone and related benzophenone derivatives

show varying cytotoxic activity profile in various cancer cell lines such as cervical cancer [12], breast cancer [13], and lung cancer [31]. This variability highlights a potential cell line-specific response, likely driven by the unique molecular landscapes of different cancer types.

Following the results of the apoptosis assay, which monitors cell death by apoptosis, showed that exposure to Chamuangone significantly induced KKU-100 cells to enter the apoptosis process in both the early and late apoptotic stages when tested for 24 and 48 hours with altering in mitochondrial membrane potential ($\Delta\psi_m$). Therefore, it can be confirmed that Chamuangone induces CCA cells death through the mechanism of programmed cell death. This finding consistency with previous reports indicating that Chamuangone and polyphenylated benzophenones from *Garcinia* species [32] can inhibit cell growth and induce apoptosis in a dose- and time-dependent manner [10]. Previous studies in HeLa cells have confirmed that Chamuangone induces

Table 6. Quantitative Analysis of Downregulated Oncogenic-Related Proteins in KKU-100 Cells after Chamuangone Treatment.

Protein expressions		Mean Pixel Density	
		Control*	Ch 3.0 $\mu\text{g/ml}$ *
1	Carbonic Anhydrase IX	41.34 \pm 24.20	0
2	Enolase2	44.96 \pm 31.63	0
3	CXCL8/IL-8	68.00 \pm 42.86	12.76 \pm 18.04
4	Galectin-3	50.64 \pm 24.40	6.24 \pm 8.82
5	EGFR/ErbB1	46.63 \pm 2.17	0
6	Progranulin	76.53 \pm 56.97	0
7	FGF basic	122.95 \pm 59.49	0
8	Dkk-1	47.01 \pm 1.55	0
9	p27/kip1	29.34 \pm 13.33	5.64 \pm 7.98
10	Mesothelin	12.50 \pm 3.10	0
11	Survivin	23.46 \pm 0.89	0

* Protein expression levels were quantified as mean pixel density normalized to internal positive controls on the array membrane (mean \pm SD).

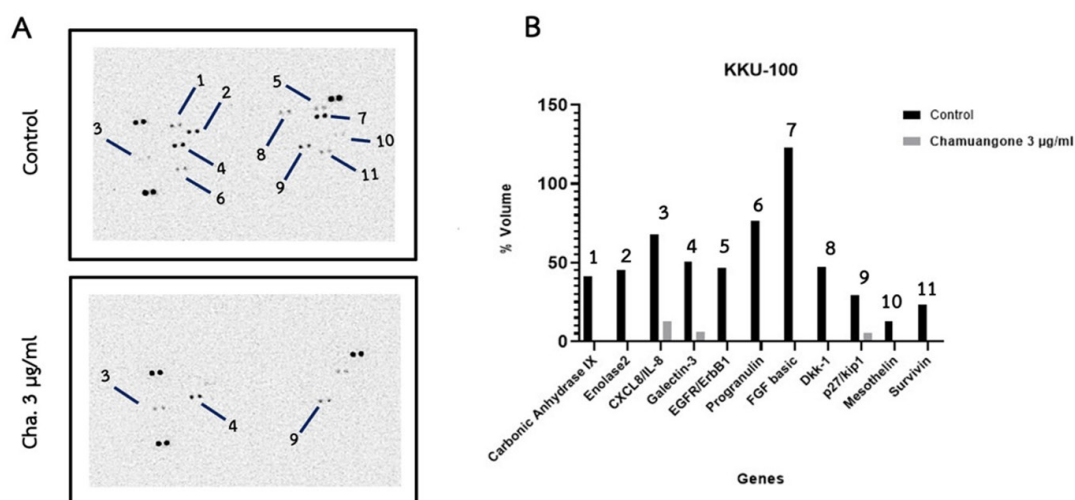


Figure 6. Effect of Chamuangone on the Expression of Cancer-Related Proteins in KKU-100 Cells. (A) Representative membrane images of protein array blots showing changes in protein spot intensities between control and Chamuangone-treated cells (3.0 $\mu\text{g/mL}$, 24 h). (B) Quantitative analysis of downregulated proteins, including Carbonic anhydrase IX, Enolase 2, CXCL8/IL-8, Galectin-3, EGFR/ErbB1, Progranulin, basic FGF, Dkk-1, p27/Kip1, Mesothelin, and Survivin, expressed as normalized mean pixel densities relative to internal positive controls.

programmed cell death via the mitochondrial pathway, characterized by a decrease in $\Delta\psi_m$ and can induce cytochrome c release subsequent activation of caspase-9 and caspase-3 [10, 33]. This mechanism is crucial for sensitizing cancer cells to chemotherapy, as it triggers the intrinsic apoptotic pathway through the activation of mitochondria-dependent signaling [34].

Additionally, *Ki67* is a nuclear protein marker that is expressed during all active phases of the cell cycle (G1, S, G2, and M phase) but is absent in quiescent cells (G0), thus serving as a standard proliferation marker [35]. In CCA, *Ki67* is frequently overexpressed and correlates with tumor grade and poor prognosis [36, 37]. The present study revealed that Chamuangone can reduce cell proliferation by increasing the proportion of cells in the resting phase (*Ki67*-negative) and decreasing the proportion of *Ki67*-positive cells, which are living and dividing cells. The reduction in *Ki67* expression reflects impaired cellular proliferative capacity and suggests an induction of cell cycle arrest at the resting phase, thereby sensitizing cells to apoptotic signal.

Subsequently, the induction of ROS supports the involvement of oxidative stress-mediated signaling in the anticancer mechanism of Chamuangone. Previous reports has been proposed that Chamuangone induces ROS generation and apoptosis in other cancer cell lines [38]. Elevated ROS levels induce oxidative stress, which damages mitochondria and DNA, ultimately leading to apoptosis [34, 39]. Natural products such as curcumin, resveratrol, quercetin and bark extract of *Phyllanthus emblica* are known to trigger ROS-mediated apoptosis through similar mechanisms [40-43]. These findings suggest that Chamuangone functions as a redox-regulated compound capable of altering the intracellular oxidative balance to induce cancer cell death that is a property of great value for the development of anticancer drugs [44].

The molecular basis underlying Chamuangone-induced oxidative stress and apoptosis involved with downregulating 11 oncogenic-related proteins. These proteins can be grouped into three main functional categories: 1) cell proliferation and survival, 2) angiogenesis and invasion, and 3) metabolic adaptation with intracellular signaling regulation.

In the first category, EGFR, survivin, progranulin, FGF-basic, and galectin-3 play crucial roles in stimulating cell growth, evading apoptosis, and mediating intracellular signaling pathways that promote cancer cell survival [45]. EGFR is predominantly expressed in the biliary duct of CCA and is closely associated with treatment outcomes and drug resistance [1, 46]. EGFR-inhibiting compounds such as gefitinib and other pharmacotherapeutic agents have been investigated for their efficacy in inducing apoptosis and sensitizing CCA cells to chemotherapy [21, 47, 48]. Another study has been reported Chamuangone exhibits stronger EGFR-tyrosine kinase inhibitory activity than gefitinib [12]. Survivin (BIRC5) is highly expressed in the bile ducts and functions as an inhibitor of apoptosis by blocking caspase-3 activation, thereby preventing programmed cell death [49]. Progranulin (PGRN) promotes tumor cell proliferation and survival through the activation of the PI3K/Akt and ERK signaling

pathways [50, 51]. FGF-basic is a key mediator of cancer cell proliferation, angiogenesis, and survival through activation of FGFR-dependent signaling pathways, including MAPK/ERK and PI3K/Akt [52, 53]. FGF-basic signaling in the bile ducts is often linked to FGFR2 alterations, which represent important therapeutic targets in intrahepatic CCA [54, 55]. FGFR2 fusions predominantly found in intrahepatic CCA patients, dictates the varying efficacy of targeted therapies and necessitates a personalized approach to treatment [56-59]. Among the downregulated proteins, FGF-basic exhibited the most reduction from a high basal expression level in control cells to nearly undetectable levels following Chamuangone treatment. Galectin-3 is highly expressed in the intrahepatic bile ducts, promoting tumor progression and enhancing anti-apoptotic activity; its inhibition has been reported to increase chemosensitivity and apoptosis [49, 60, 61]. Collectively, these findings underscore that Chamuangone strongly interferes with growth factor-driven oncogenic signaling, which may further sensitize CCA cells to oxidative stress and induce apoptosis.

In the second category, IL-8, CAIX, FGF-basic, and Mesothelin [62]. IL-8 acts as a pro-angiogenic cytokine that promotes endothelial cell migration and is strongly associated with tumor progression and metastasis in cholangiocarcinoma [63, 64]. CAIX (Carbonic Anhydrase IX) is overexpressed under hypoxic conditions and is correlated with tumor aggressiveness and metastatic potential in cholangiocarcinoma [65, 66]. Mesothelin facilitates cancer cell adhesion and peritoneal metastasis, serving as a diagnostic and therapeutic biomarker in biliary tract cancers [67]. The decreased levels of these proteins following Chamuangone treatment suggest that this compound may inhibit angiogenesis and reduce cancer cell metastasis.

In the third category, Enolase 2, Dkk-1, and p27 are glycolytic enzyme that enhances energy production in cancer cells [68]. Dkk-1 acts as a regulator of Wnt/ β -catenin signaling and promotes metastasis in gastrointestinal and biliary tract cancers [69, 70]. P27/Kip1, a cyclin-dependent kinase inhibitor, is frequently downregulated in cholangiocarcinoma, leading to uncontrolled cell proliferation and tumor progression [71-73]. Downregulation of these proteins following Chamuangone exposure suggests a disturbance in glycolytic reprogramming, which is critical to tumor metabolic adaptation [74]. Metabolic reprogramming, particularly the glycolytic transition and mitochondrial stress, is increasingly recognized as a hallmark of CCA progression [75]. The reduction in these proteins after Chamuangone exposure might reflect disruption of signaling and metabolic pathways essential for cancer growth.

The interplay of these three protein groups is directly linked to oxidative stress, as increased ROS affects EGFR and FGF basic signaling, induces CAIX expression, and disrupts energy metabolism [15, 76, 77]. Therefore, the simultaneous decrease in these proteins after Chamuangone treatment reflects a systematic inhibition of redox-responsive cancer gene networks [77].

FGF-basic and EGFR were significantly downregulated, which is a key feature, as they are major drivers of CCA [15, 78]. The inhibition of these two proteins suggests that Chamuangone may play a dual-pathway inhibitory role, indicating a high potential for future anticancer drug development [79]. Overall, the decreased levels of proteins across all three groups after Chamuangone treatment demonstrate that this compound exerts anticancer effects by simultaneously targeting multiple processes, including cell growth and survival, angiogenesis, and metabolic adaptation [15, 80]. The underlying mechanisms include the stimulation of ROS generation, the loss of mitochondrial membrane potential, and the inhibition of the EGFR and FGF basic signaling pathway, leading to decreased cell proliferation and increased apoptosis. These results are consistent with previous reports indicating that Chamuangone and polyphenylated benzophenones from *Garcinia* exert tumor-suppressive effects via oxidative stress-dependent apoptosis induction and growth factor signaling inhibition [13, 15, 80]

In conclusion, Chamuangone demonstrates significant potential as a novel anticancer drug prototype by targeting multiple oncogenic signaling pathways and disrupting redox homeostasis, leading to excessive ROS accumulation, mitochondrial dysfunction, and activation of apoptotic cell death pathways. This broad suppression of oncogenic and redox-regulating mechanisms highlights Chamuangone as a promising multi-target anticancer agent for the treatment of CCA.

Author Contribution Statement

W.T.: Principal investigator; performed the experiments and data analysis; original draft preparation; review and editing. T.S.: Assisted with the experiments; writing and review. B.S.: Methodology for MTT assay. S.L.: Methodology for apoptosis analysis. P.C.: Formal analysis and validation. S.K. and K.C.: supervision. P.P.: Extraction and Purification of Chamuangone from *Garcinia cowa* Leaves. P.S.: Writing-review and editing; project administration; conceptualization; funding acquisition, formal analysis and validation. All authors have read and approved the final version of the manuscript for publication.

Acknowledgements

This study was financially supported by the Faculty of Medicine, Srinakharinwirot University (Grant Nos. 274/2568 and 275/2568). The authors gratefully acknowledge Dr. James R. Smith, School of Pharmacy and Biomedical Sciences, University of Portsmouth, UK, for assistance with English language editing and valuable comments on the manuscript. The authors also acknowledge the Faculty of Medicine, Srinakharinwirot University, for providing research facilities and technical support.

Ethics Approval Statement

This study was reviewed and approved by the Ethics Committee of Srinakharinwirot University (Approval No.

SWUEC-683069).

Declaration of Generative AI and AI-Assisted Technologies in the manuscript preparation process

Generative AI (ChatGPT) was used to improve English grammar and language during manuscript preparation. The authors reviewed and edited the content and took full responsibility for the published work.

Conflicts of Interest

The authors declare no conflict of interest.

References

1. Banales JM, Marin JJG, Lamarca A, Rodrigues PM, Khan SA, Roberts LR, et al. Cholangiocarcinoma 2020: The next horizon in mechanisms and management. *Nat Rev Gastroenterol Hepatol*. 2020;17(9):557-88. <https://doi.org/10.1038/s41575-020-0310-z>.
2. Plieskatt JL, Deenonpoe R, Mulvenna JP, Krause L, Sripa B, Bethony JM, et al. Infection with the carcinogenic liver fluke *opisthorchis viverrini* modifies intestinal and biliary microbiome. *Faseb J*. 2013;27(11):4572-84. <https://doi.org/10.1096/fj.13-232751>.
3. Ilyas SI, Gores GJ. Pathogenesis, diagnosis, and management of cholangiocarcinoma. *Gastroenterology*. 2013;145(6):1215-29. <https://doi.org/10.1053/j.gastro.2013.10.013>.
4. Liu Q, Chen Y, Hu Y, Yang J. Clinical research progress of targeted therapy combined with immunotherapy for advanced cholangiocarcinoma. *Cancer Treat Res Commun*. 2023;37:100771. <https://doi.org/10.1016/j.ctarc.2023.100771>.
5. Jang JS, Lim HY, Hwang IG, Song HS, Yoo N, Yoon S, et al. Gemcitabine and oxaliplatin in patients with unresectable biliary cancer including gall bladder cancer: A Korean cancer study group phase ii trial. *Cancer Chemother Pharmacol*. 2010;65(4):641-7. <https://doi.org/10.1007/s00280-009-1069-7>.
6. Zheng Q, Zhang B, Li C, Zhang X. Overcome drug resistance in cholangiocarcinoma: New insight into mechanisms and refining the preclinical experiment models. *Front Oncol*. 2022;12:850732. <https://doi.org/10.3389/fonc.2022.850732>.
7. Gu Y, Yang R, Zhang Y, Guo M, Takehiro K, Zhan M, et al. Molecular mechanisms and therapeutic strategies in overcoming chemotherapy resistance in cancer. *Mol Biomed*. 2025;6(1):2. <https://doi.org/10.1186/s43556-024-00239-2>.
8. Marin JJG, Sanchon-Sanchez P, Cives-Losada C, Del Carmen S, González-Santiago JM, Monte MJ, et al. Novel pharmacological options in the treatment of cholangiocarcinoma: Mechanisms of resistance. *Cancers (Basel)*. 2021;13(10). <https://doi.org/10.3390/cancers13102358>.
9. Changprasert S, Tongtao S, Noppornphan C, Somsri S. 25 Value addition of a local food using *Garcinia cowa* leaves through collective action and marketing by a women's group. *Tropical Fruit Tree Diversity*. 2016 May 12:310.
10. Sae-lim p, yuenyongsawad s, panichayupakaranant p. Chamuangone-enriched *Garcinia cowa* leaf extract with rice bran oil: Extraction and cytotoxic activity against cancer cells. *Pharmacogn mag*. 2019;15(61):183-88. https://doi.org/10.4103/pm.pm_472_18.
11. Rahman AU, Panichayupakaranant P. Exploring the diverse biological activities of *Garcinia cowa*: implications for future cancer chemotherapy and beyond. *Food Bioscience*. 2024 Oct 1;61:104525.
12. Sae-Lim P, Seetaha S, Tabtimmai L, Suphakun P, Kiriwan

- D, Panichayupakaranant P, et al. Chamuangone from garcinia cowa leaves inhibits cell proliferation and migration and induces cell apoptosis in human cervical cancer in vitro. *J Pharm Pharmacol*. 2020;72(3):470-80. <https://doi.org/10.1111/jph.13216>.
13. Rahman AU, Khan NU, Ni J, Panichayupakaranant P. Antimetastatic effects of chamuangone-enriched extract in breast cancer lung metastasis: In vitro and in vivo evidence. *Med Oncol*. 2025;42(11):517. <https://doi.org/10.1007/s12032-025-03076-7>.
 14. Sakunpak A, Matsunami K, Otsuka H, Panichayupakaranant P. Isolation of chamuangone, a cytotoxic compound against Leishmania major and cancer cells from Garcinia cowa leaves and its HPLC quantitative determination method. *Journal of Cancer Research Updates*. 2017 Apr 12;6(2):38-45.
 15. Asad Ur R, Naveed Ullah K, Pharkphoom P, Jiang N. A standardized chamuangone enriched extract shows anticancer efficacy in allograft models of metastatic breast cancer. *J Funct Foods*. 2025;127:106730. <https://doi.org/https://doi.org/10.1016/j.jff.2025.106730>.
 16. Sripa B, Leungwattanawanit S, Nitta T, Wongkham C, Bhudhisawasdi V, Puapairoj A, et al. Establishment and characterization of an opisthorchiasis-associated cholangiocarcinoma cell line (kku-100). *World J Gastroenterol*. 2005;11(22):3392-7. <https://doi.org/10.3748/wjg.v11.i22.3392>.
 17. Saensa-Ard S, Leuangwattanawanit S, Senggunprai L, Namwat N, Kongpetch S, Chamgramol Y, et al. Establishment of cholangiocarcinoma cell lines from patients in the endemic area of liver fluke infection in thailand. *Tumour Biol*. 2017;39(11):1010428317725925. <https://doi.org/10.1177/1010428317725925>.
 18. Jantalika T, Manochantr S, Kheolamai P, Tantikanlayaporn D, Pinlaor S, Saijuntha W, et al. Human chorion and placental mesenchymal stem cells conditioned media suppress cell migration and invasion by inhibiting the pi3k/akt pathway in cholangiocarcinoma. *Sci Rep*. 2025;15(1):31472. <https://doi.org/10.1038/s41598-025-16789-6>.
 19. Seubwai W, Wongkham C, Puapairoj A, Khuntikeo N, Pugkhem A, Hahnvajanawong C, et al. Aberrant expression of nf-kb in liver fluke associated cholangiocarcinoma: Implications for targeted therapy. *PLoS One*. 2014;9(8):e106056. <https://doi.org/10.1371/journal.pone.0106056>.
 20. Samatiwat P, Prawan A, Senggunprai L, Kukongviriyapan U, Kukongviriyapan V. Nrf2 inhibition sensitizes cholangiocarcinoma cells to cytotoxic and antiproliferative activities of chemotherapeutic agents. *Tumour Biol*. 2016;37(8):11495-507. <https://doi.org/10.1007/s13277-016-5015-0>.
 21. Samatiwat P, Tabtimmai L, Suphakun P, Jiwacharoenchai N, Toviwek B, Kukongviriyapan V, et al. The effect of the egfr - targeting compound 3-[(4-phenylpyrimidin-2-yl) amino] benzene-1-sulfonamide (13f) against cholangiocarcinoma cell lines. *Asian Pac J Cancer Prev*. 2021;22(2):381-90. <https://doi.org/10.31557/apjcp.2021.22.2.381>.
 22. Ghasemi M, Turnbull T, Sebastian S, Kempson I. The mt assay: Utility, limitations, pitfalls, and interpretation in bulk and single-cell analysis. *Int J Mol Sci*. 2021;22(23). <https://doi.org/10.3390/ijms222312827>.
 23. Lakshmanan I, Batra SK. Protocol for apoptosis assay by flow cytometry using annexin v staining method. *Bio Protoc*. 2013;3(6). <https://doi.org/10.21769/bioprotoc.374>.
 24. Eminaga S, Teekakirikul P, Seidman CE, Seidman JG. Detection of cell proliferation markers by immunofluorescence staining and microscopy imaging in paraffin-embedded tissue sections. *Curr Protoc Mol Biol*. 2016;115:14.25.1-14.25.14. <https://doi.org/10.1002/cpmb.13>.
 25. Sivandzade F, Bhalerao A, Cucullo L. Analysis of the mitochondrial membrane potential using the cationic jc-1 dye as a sensitive fluorescent probe. *Bio Protoc*. 2019;9(1). <https://doi.org/10.21769/BioProtoc.3128>.
 26. Murphy MP, Bayir H, Belousov V, Chang CJ, Davies KJA, Davies MJ, et al. Guidelines for measuring reactive oxygen species and oxidative damage in cells and in vivo. *Nat Metab*. 2022;4(6):651-62. <https://doi.org/10.1038/s42255-022-00591-z>.
 27. Kiss T, Jámbor K, Koroknai V, Szász I, Bárdos H, Mokánszki A, et al. Silencing osteopontin expression inhibits proliferation, invasion and induce altered protein expression in melanoma cells. *Pathol Oncol Res*. 2021;27:581395. <https://doi.org/10.3389/pore.2021.581395>.
 28. Fraveto A, Cardinale V, Bragazzi MC, Giuliani F, De Rose AM, Grazi GL, et al. Sensitivity of human intrahepatic cholangiocarcinoma subtypes to chemotherapeutics and molecular targeted agents: A study on primary cell cultures. *PLoS One*. 2015;10(11):e0142124. <https://doi.org/10.1371/journal.pone.0142124>.
 29. Hong JH, Lim AH, Kaewnarin K, Chan JY, Ng CCY, Teh BT. Biodiversity medicine: New horizon and new opportunity for cancer. *Cancer Discov*. 2024;14(3):392-5. <https://doi.org/10.1158/2159-8290.Cd-23-1585>.
 30. Bai M, Wang R, Huang C, Zhong R, Jiang N, Fu W, et al. Biological and genetic characterization of a newly established human primary multidrug-resistant distal cholangiocarcinoma cell line, cbc3t-6. *Sci Rep*. 2024;14(1):29661. <https://doi.org/10.1038/s41598-024-81392-0>.
 31. Wanaragthai P, Yingchutrakul Y, Panichayupakaranant P, Vongsvivut J, Aonbangkhen C, Yang MC, et al. Integrated synchrotron radiation-based fourier transform infrared (sr-ftir) microscopy and tandem-mass spectrometry (lc-ms/ms) used to elucidate the apoptotic effect of chamuangone in a549 cells. *Biochem Biophys Res Commun*. 2025;764:151826. <https://doi.org/10.1016/j.bbrc.2025.151826>.
 32. Senthilkumar HA. Anti-proliferative Effects of Garcinia Fruits in Breast Cancer Cells. City University of New York; 2018.
 33. Hui Z, Juan W, Dan L, Zhijun Z, Ruirong Y, Rongtao L, et al. Bioactive dihydroagarofuran sesquiterpenes from the twigs of tripterygium hypoglaucom. *Phytochem Lett*. 2021;41:92-100. <https://doi.org/10.1016/j.phytol.2020.10.011>.
 34. Sinha K, Das J, Pal PB, Sil PC. Oxidative stress: The mitochondria-dependent and mitochondria-independent pathways of apoptosis. *Arch Toxicol*. 2013;87(7):1157-80. <https://doi.org/10.1007/s00204-013-1034-4>.
 35. Kaunda JS, Zhang YJ. The genus solanum: An ethnopharmacological, phytochemical and biological properties review. *Nat Prod Bioprospect*. 2019;9(2):77-137. <https://doi.org/10.1007/s13659-019-0201-6>.
 36. Ogasawara Y, Yoshitomi S, Sato S, Doihara H. Clinical significance of preoperative lymphoscintigraphy for sentinel lymph node biopsy in breast cancer. *J Surg Res*. 2008;148(2):191-6. <https://doi.org/10.1016/j.jss.2007.10.022>.
 37. Castanon A, Landy R, Lim AW, Sasieni P. Response to comment on 'characteristics and screening history of women diagnosed with cervical cancer aged 20-29'. *Br J Cancer*. 2014;111(12):2374. <https://doi.org/10.1038/bjc.2014.465>.
 38. Saidi L, Rocha DHA, Talhi O, Bentarzi Y, Nedjar-Kolli B, Bachari K, et al. Synthesis of benzophenones and in vitro evaluation of their anticancer potential in breast and prostate cancer cells. *ChemMedChem*. 2019;14(10):1041-8. <https://doi.org/10.1002/cmdc.201900411>.

- doi.org/10.1002/cmde.201900127.
39. Zhao Y, Ye X, Xiong Z, Ihsan A, Ares I, Martínez M, et al. Cancer metabolism: The role of ros in DNA damage and induction of apoptosis in cancer cells. *Metabolites*. 2023;13(7). <https://doi.org/10.3390/metabo13070796>.
 40. Cecerska-Heryć E, Wiśniewska Z, Serwin N, Polikowska A, Goszka M, Engwert W, et al. Can compounds of natural origin be important in chemoprevention? Anticancer properties of quercetin, resveratrol, and curcumin—a comprehensive review. *Int J Mol Sci*. 2024;25(8). <https://doi.org/10.3390/ijms25084505>.
 41. Hasan AA, Tatarskiy V, Kalinina E. Synthetic pathways and the therapeutic potential of quercetin and curcumin. *Int J Mol Sci*. 2022;23(22). <https://doi.org/10.3390/ijms232214413>.
 42. Biswas P, Dey D, Biswas PK, Rahaman TI, Saha S, Parvez A, et al. A comprehensive analysis and anti-cancer activities of quercetin in ros-mediated cancer and cancer stem cells. *Int J Mol Sci*. 2022;23(19). <https://doi.org/10.3390/ijms231911746>.
 43. Samatiwat P, Chankhonkaen P, Jaisin Y, Ratanachamnong P, Niwaspragrit C, Rungsriwut R. Anticancer activity of the bark extract of *Phyllanthus emblica* on cholangiocarcinoma in vitro. *J Basic Appl Pharmacology*. 2021;1(1):60-71.
 44. Bansal MP. ROS, redox regulation, and anticancer therapy. Redox regulation and therapeutic approaches in cancer: Springer; 2023. P. 311-409.
 45. Kiss T. The role of osteopontin expression during malignant melanoma progression (Doctoral dissertation, Debreceni Egyetem (Hungary)); 2023.
 46. Yoshikawa D, Ojima H, Iwasaki M, Hiraoka N, Kosuge T, Kasai S, et al. Clinicopathological and prognostic significance of egfr, vegf, and her2 expression in cholangiocarcinoma. *Br J Cancer*. 2008;98(2):418-25. <https://doi.org/10.1038/sj.bjc.6604129>.
 47. Nakajima Y, Takagi H, Kakizaki S, Horiguchi N, Sato K, Sunaga N, et al. Gefitinib and gemcitabine coordinately inhibited the proliferation of cholangiocarcinoma cells. *Anticancer Res*. 2012;32(12):5251-62.
 48. Francis H, Alpini G, DeMorrow S. Recent advances in the regulation of cholangiocarcinoma growth. *Am J Physiol Gastrointest Liver Physiol*. 2010;299(1):G1-9. <https://doi.org/10.1152/ajpgi.00114.2010>.
 49. Li F, Aljhdali I, Ling X. Cancer therapeutics using survivin birc5 as a target: What can we do after over two decades of study? *J Exp Clin Cancer Res*. 2019;38(1):368. <https://doi.org/10.1186/s13046-019-1362-1>.
 50. Zhou C, Huang Y, Wu J, Wei Y, Chen X, Lin Z, et al. A narrative review of multiple mechanisms of progranulin in cancer: A potential target for anti-cancer therapy. *Transl Cancer Res*. 2021;10(9):4207-16. <https://doi.org/10.21037/tcr-20-2972>.
 51. Yang D, Wang LL, Dong TT, Shen YH, Guo XS, Liu CY, et al. Progranulin promotes colorectal cancer proliferation and angiogenesis through tnfr2/akt and erk signaling pathways. *Am J Cancer Res*. 2015;5(10):3085-97.
 52. Ardizzone A, Bova V, Casili G, Repici A, Lanza M, Giuffrida R, et al. Role of basic fibroblast growth factor in cancer: Biological activity, targeted therapies, and prognostic value. *Cells*. 2023;12(7). <https://doi.org/10.3390/cells12071002>.
 53. Du S, Zhang Y, Xu J. Current progress in cancer treatment by targeting fgfr signaling. *Cancer Biol Med*. 2023;20(7):490-9. <https://doi.org/10.20892/j.issn.2095-3941.2023.0137>.
 54. Goyal L, Meric-Bernstam F, Hollebecque A, Valle JW, Morizane C, Karasic TB, et al. Futibatinib for fgfr2-rearranged intrahepatic cholangiocarcinoma. *N Engl J Med*. 2023;388(3):228-39. <https://doi.org/10.1056/NEJMoa2206834>.
 55. Vogel A, Segatto O, Stenzinger A, Saborowski A. Fgfr2 inhibition in cholangiocarcinoma. *Annu Rev Med*. 2023;74:293-306. <https://doi.org/10.1146/annurev-med-042921-024707>.
 56. Borad MJ, Gores GJ, Roberts LR. Fibroblast growth factor receptor 2 fusions as a target for treating cholangiocarcinoma. *Curr Opin Gastroenterol*. 2015;31(3):264-8. <https://doi.org/10.1097/mog.0000000000000171>.
 57. Goyal L, Kongpetch S, Crolley VE, Bridgewater J. Targeting fgfr inhibition in cholangiocarcinoma. *Cancer Treat Rev*. 2021;95:102170. <https://doi.org/10.1016/j.ctrv.2021.102170>.
 58. Shen L, Duan H, Kuwahara T, Satoh T, Ma X, Yan S, et al. Tasurgratinib (e7090) for cholangiocarcinoma with fibroblast growth factor receptor 2 fusions/rearrangements: A multicenter, open-label, phase 2 study. *Jpn J Clin Oncol*. 2025;55(11):1229-36. <https://doi.org/10.1093/jjco/hyaf119>.
 59. Szymczyk J, Sluzalska KD, Materla I, Opalinski L, Otlewski J, Zakrzewska M. Fgf/fgfr-dependent molecular mechanisms underlying anti-cancer drug resistance. *Cancers (Basel)*. 2021;13(22). <https://doi.org/10.3390/cancers13225796>.
 60. Wongkham S, Junking M, Wongkham C, Sripa B, Chur-In S, Araki N. Suppression of galectin-3 expression enhances apoptosis and chemosensitivity in liver fluke-associated cholangiocarcinoma. *Cancer Sci*. 2009;100(11):2077-84. <https://doi.org/10.1111/j.1349-7006.2009.01304.x>.
 61. Li H, Li J, Xiao W, Zhang Y, Lv Y, Yu X, et al. The therapeutic potential of galectin-3 in the treatment of intrahepatic cholangiocarcinoma patients and those compromised with covid-19. *Front Mol Biosci*. 2021;8:666054. <https://doi.org/10.3389/fmolb.2021.666054>.
 62. Caligiuri A, Pastore M, Lori G, Raggi C, Di Maira G, Marra F, et al. Role of chemokines in the biology of cholangiocarcinoma. *Cancers (Basel)*. 2020;12(8). <https://doi.org/10.3390/cancers12082215>.
 63. Rizzo M, Varnier L, Pezzicoli G, Pirovano M, Cosmai L, Porta C. Il-8 and its role as a potential biomarker of resistance to anti-angiogenic agents and immune checkpoint inhibitors in metastatic renal cell carcinoma. *Front Oncol*. 2022;12:990568. <https://doi.org/10.3389/fonc.2022.990568>.
 64. Zhang N, Shu L, Liu Z, Shi A, Zhao L, Huang S, et al. The role of extracellular vesicles in cholangiocarcinoma tumor microenvironment. *Front Pharmacol*. 2023;14:1336685. <https://doi.org/10.3389/fphar.2023.1336685>.
 65. Pastorek J, Pastorekova S. Hypoxia-induced carbonic anhydrase ix as a target for cancer therapy: From biology to clinical use. *Seminars in cancer biology*; Elsevier: 2015.
 66. Pastorekova S, Gillies RJ. The role of carbonic anhydrase ix in cancer development: Links to hypoxia, acidosis, and beyond. *Cancer Metastasis Rev*. 2019;38(1-2):65-77. <https://doi.org/10.1007/s10555-019-09799-0>.
 67. Ellinghaus P, Neureiter D, Nogai H, Stintzing S, Ocker M. Patient selection approaches in fgfr inhibitor trials—many paths to the same end? *Cells*. 2022;11(19). <https://doi.org/10.3390/cells11193180>.
 68. Jiang H. Prostate cancer bone metastasis: Molecular mechanisms of tumor and bone microenvironment. *Cancer Manag Res*. 2025;17:219-37. <https://doi.org/10.2147/cmar.S495169>.
 69. Zhu G, Song J, Chen W, Yuan D, Wang W, Chen X, et al. Expression and role of dickkopf-1 (dkk1) in tumors: From the cells to the patients. *Cancer Manag Res*. 2021;13:659-75. <https://doi.org/10.2147/cmar.S275172>.
 70. Liang L, He H, Lv R, Zhang M, Huang H, An Z, et al. Preliminary mechanism on the methylation modification of dkk-1 and dkk-3 in hepatocellular carcinoma. *Tumour Biol*. 2015;36(2):1245-50. <https://doi.org/10.1007/s13277-014-2750-y>.

71. Zheng J, Li Q, Wang W, Wang Y, Fu X, Wang W, et al. Apoptosis-related protein-1 acts as a tumor suppressor in cholangiocarcinoma cells by inducing cell cycle arrest via downregulation of cyclin-dependent kinase subunits. *Oncol Rep.* 2016;35(2):809-16. <https://doi.org/10.3892/or.2015.4422>.
72. Chen R, He F, He H, York JP, Liu W, Xia X. Phosphorylation of p27 by akt is required for inhibition of cell cycle progression in cholangiocarcinoma. *Dig Liver Dis.* 2018;50(5):501-6. <https://doi.org/10.1016/j.dld.2017.12.021>.
73. Huang J, Yang W, Jiang K, Liu Y, Tan X, Luo J. Rnf4 promotes tumorigenesis, therapy resistance of cholangiocarcinoma and affects cell cycle by regulating the ubiquitination degradation of p27kip1 in the nucleus. *Exp Cell Res.* 2022;419(1):113295. <https://doi.org/10.1016/j.yexcr.2022.113295>.
74. Chiu CF, Guerrero JGG, Regalado RRH, Zhou J, Notarte KI, Lu YW, et al. Insights into metabolic reprogramming in tumor evolution and therapy. *Cancers (Basel).* 2024;16(20). <https://doi.org/10.3390/cancers16203513>.
75. Qin H, Zheng G, Li Q, Shen L. Metabolic reprogramming induced by dca enhances cisplatin sensitivity through increasing mitochondrial oxidative stress in cholangiocarcinoma. *Front Pharmacol.* 2023;14:1128312. <https://doi.org/10.3389/fphar.2023.1128312>.
76. Rahman AU, Khan NU, Khan M, Khan ZU, Basit A, Panichayupakaranant P. A standardized chamuangone enriched extract from *garcinia cowa roxb.* Leaves shows acute and sub-acute safety. *J Ethnopharmacol.* 2024;335:118625. <https://doi.org/10.1016/j.jep.2024.118625>.
77. Weng MS, Chang JH, Hung WY, Yang YC, Chien MH. The interplay of reactive oxygen species and the epidermal growth factor receptor in tumor progression and drug resistance. *J Exp Clin Cancer Res.* 2018;37(1):61. <https://doi.org/10.1186/s13046-018-0728-0>.
78. Kaur N, Gare SR, Shen J, Raja R, Fonseka O, Liu W. Multi-organ fgf21-fgfr1 signaling in metabolic health and disease. *Front Cardiovasc Med.* 2022;9:962561. <https://doi.org/10.3389/fcvm.2022.962561>.
79. Jantarawong S, Wathanaphanit P, Panichayupakaranant P, Pengjam Y. Prediction of admet profile and anti-inflammatory potential of chamuangone. *Sci Rep.* 2025;15(1):2963. <https://doi.org/10.1038/s41598-025-86809-y>.
80. Rahman AU, Khan NU, Basit A, Khan M, Ni J, Panichayupakaranant P. Chamuangone purified from *garcinia cowa* inhibits inflammation, angiogenesis, epithelial-mesenchymal transition, and metastasis in breast cancer. *J Sci Food Agric.* 2026;106(1):469-81. <https://doi.org/10.1002/jsfa.70175>.



This work is licensed under a Creative Commons Attribution-Non Commercial 4.0 International License.